

Latent Diffusion for Language Generation

Justin Lovelace Varsha Kishore Chao Wan Eliot Shekhtman Kilian Weinberger
 Cornell University
 {jl3353, vk352, cw862, ess239, kqw4}@cornell.edu

Abstract

Diffusion models have achieved great success in modeling continuous data modalities such as images, audio, and video, but have seen limited use in discrete domains such as language. Recent attempts to adapt diffusion to language have presented diffusion as an alternative to autoregressive language generation. We instead view diffusion as a complementary method that can augment the generative capabilities of existing pre-trained language models. We demonstrate that continuous diffusion models can be learned in the latent space of a pre-trained encoder-decoder model, enabling us to sample continuous latent representations that can be decoded into natural language with the pre-trained decoder. We show that our latent diffusion models are more effective at sampling novel text from data distributions than a strong autoregressive baseline and also enable controllable generation.

1 Introduction

Diffusion models (Sohl-Dickstein et al., 2015; Ho et al., 2020) are a class of latent variable models that learn to gradually transform random noise drawn from a Gaussian distribution, which can be sampled analytically, to a sample from an unknown data distribution specified by a collection of samples. This class of generative models has recently achieved widespread success with continuous data modalities such as images (Ho et al., 2020), audio (Kong et al., 2021), and video (Ho et al., 2022). Diffusion models have also seen great success in controllable generation and underlying state-of-the-art text-to-image systems such as Dalle-2 (Ramesh et al., 2022) and Imagen (Saharia et al., 2022).

Language generation, on the other hand, is currently dominated by large autoregressive transformers (Brown et al., 2020). While such models have

demonstrated impressive performance across a variety of language generation tasks, eliciting desired behaviors from such models is challenging and often requires careful prompt engineering (Perez et al., 2021).

The success of diffusion models in controllable generation makes them appealing for language generation. However, so far they have seen limited use in such discrete domains, where the gradual transition of discrete states to Gaussian noise (and vice versa) is not as natural as in continuous domains like natural images. Prior work has defined diffusion processes over discrete state spaces in an attempt to model discrete data directly (Hoogendoorn et al., 2021; Austin et al., 2021), but these approaches have lagged behind continuous diffusion models.

Other work (Li et al., 2022; Strudel et al., 2022) has learned continuous diffusion models directly in the space of word embeddings and decode the continuous generations with a rounding step. Such work has presented diffusion models as a potential alternative to autoregressive language models.

In contrast, we present diffusion as a complementary tool to autoregressive generation, rather than a replacement. We demonstrate that a continuous diffusion model can be learned in the latent space of a pre-trained encoder-decoder language model. The continuous vectors sampled from the diffusion model can then be decoded into natural language by the pre-trained decoder. In doing so, we side-step the challenge of directly modeling a discrete distribution with diffusion and enable the use of continuous methods for natural language.

We find that our latent diffusion model is effective for both unconditional and conditional language generation across a variety of datasets. In particular, we show that our approach is more effective at generating novel text from a data distribution than a pre-trained GPT2 model of a similar scale.

Code is available at <https://github.com/justinlovelace/latent-diffusion-for-language>

2 Related Work

Autoregressive Language Models. Autoregressive transformer models such as GPT-3 (Brown et al., 2020) and PaLM (Chowdhery et al., 2022) are the current state-of-the-art for language modeling and have achieved impressive few-shot and zero-shot performance across a wide range of language tasks and on open-ended text generation.

Diffusion models. Diffusion models (Sohl-Dickstein et al., 2015; Ho et al., 2020) are a class of generative models that have led to impressive results in image synthesis, recently surpassing Generative Adversarial Networks (Goodfellow et al., 2014; Dhariwal and Nichol, 2021). These models typically operate directly in pixel-space, learning a distribution over images.

Latent Diffusion. Rombach et al. (2022) introduced latent diffusion models for image synthesis and demonstrated that diffusion models can be learned in the latent space of a pre-trained image autoencoder. At inference time, the generative process produces samples from the image autoencoder’s latent space which can be decoded to pixel space with the decoder.

Diffusion for Language. Li et al. (2022) train a continuous diffusion model in the space of token embeddings that are learned jointly with the denoising objective. Their approach enables controlling attributes like the length, sentiment, syntactic structure, or semantic content of generated language. Strudel et al. (2022) scaled up this approach and found the joint training scheme to be unstable. They instead learned the diffusion model in the space of pre-trained word embeddings. However, they found that diffusion scaled poorly to high-dimensional word embeddings.

Chen et al. (2022) mapped words to arbitrary binary strings, represented as a sequence of real numbers. They then train a continuous diffusion model and round the generated sequences to produce binary strings. The authors also introduce self-conditioning, a technique that conditions the diffusion model on its prediction from prior steps. Their model improved upon existing discrete diffusion models, but binary representations fail to capture a notion of similarity between words.

3 Background on Diffusion Models

Diffusion models attempt to approximate some unknown data distribution, $p(\mathbf{x})$, to enable useful operations like sampling from that distribution for data generation. Instead of attempting to model $p(\mathbf{x})$ directly like auto-regressive language models (Brown et al., 2020), diffusion models learn a mapping between a Gaussian distribution, where sampling is easy, and the data distribution, where sampling is hard. This mapping is defined through a forward process that iteratively adds Gaussian noise to samples from the data distribution, and a generative process that iteratively “denoises” samples from the Gaussian distribution to obtain samples from the data distribution as discussed below.

3.1 Forward Process

Diffusion models first define a transition, known as the forward diffusion process, from the data to a Gaussian distribution. Given a data sample, $\mathbf{x} \in \mathbb{R}^d \sim p(\mathbf{x})$, the forward process introduces latent variables $\{\mathbf{z}_0, \mathbf{z}_1, \dots, \mathbf{z}_T\}$ that gradually interpolate between the data distribution and a Gaussian distribution as the timesteps increase.

The process starts with the original data point $\mathbf{z}_0 = \mathbf{x} \sim p(\mathbf{x})$ and at each iteration, t , adds more noise from a Gaussian distribution. More formally, the forward process can be described as a Markov chain parameterized with some variances β_t

$$q(\mathbf{z}_{1:T} | \mathbf{z}_0) = \prod_{t=1}^T q(\mathbf{z}_t | \mathbf{z}_{t-1}), \quad (1)$$

where $q(\mathbf{z}_t | \mathbf{z}_{t-1}) \sim \mathcal{N}(\sqrt{1 - \beta_t} \mathbf{z}_{t-1}, \beta_t \mathbf{I})$.

Because iteratively adding Gaussian noise is identical to adding Gaussian noise once, with a higher variance, the forward process has the convenient property that for any time t , $q(\mathbf{z}_t | \mathbf{x})$ is also Gaussian and has a closed-form solution. It can be written in terms of a scalar $\alpha_t = \prod_{i=1}^t (1 - \beta_i)$ as

$$\begin{aligned} \mathbf{z}_t \sim q(\mathbf{z}_t | \mathbf{x}) &= \mathcal{N}(\sqrt{\alpha_t} \mathbf{x}, (1 - \alpha_t) \mathbf{I}) \iff \\ \mathbf{z}_t &= \sqrt{\alpha_t} \mathbf{x} + \sqrt{1 - \alpha_t} \boldsymbol{\epsilon}, \boldsymbol{\epsilon} \sim \mathcal{N}(0, \mathbf{I}). \end{aligned} \quad (2)$$

The noise schedule, represented through $\alpha_t \in (0, 1)$, is defined such that $(1 - \alpha_t)$ increases monotonically from $(1 - \alpha_1) \approx 0$ to $(1 - \alpha_T) \approx 1$.

As a result, the latent variable is initially close to the data, i.e. $\mathbf{z}_1 \sim q(\mathbf{z}_1 | \mathbf{x}) \approx \mathbf{x}$. As t increases, the latents become noisier until the final vector \mathbf{z}_T is approximately Gaussian, $\mathbf{z}_T \sim q(\mathbf{z}_T | \mathbf{x}) \approx \mathcal{N}(0, 1)$ — independent from the starting point \mathbf{x} .

3.2 Generative Process

We obtain our generative process by inverting the forward Markov chain. For generation, we treat Gaussian noise as corrupted data, $\mathbf{z}_T \sim \mathcal{N}(0, 1)$, that we iteratively “denoise” to obtain increasingly structured latents, $\mathbf{z}_{T-1}, \mathbf{z}_{T-2}, \dots, \mathbf{z}_0$, such that \mathbf{z}_0 is an approximate sample from the data distribution. Therefore, our learnable generative process is defined by the inverted Markov chain $p_\theta(\mathbf{z}_{0:T}) = p(\mathbf{z}_T) \prod_{t=1}^T p_\theta(\mathbf{z}_{t-1} | \mathbf{z}_t)$. By design, the start, $p(\mathbf{z}_T) = \mathcal{N}(0, 1)$, is easy to sample from.

To define $p_\theta(\mathbf{z}_{t-1} | \mathbf{z}_t)$ we utilize the property that, given access to the original data \mathbf{x} , the forward process can be inverted analytically. This inversion is given as,

$$q(\mathbf{z}_{t-1} | \mathbf{z}_t, \mathbf{x}) = \mathcal{N}(\mu_t(\mathbf{z}_t, \mathbf{x}), \sigma_t^2 \mathbf{I}), \quad (3)$$

where $\mu_t(\mathbf{z}_t, \mathbf{x})$ has a closed-form solution and σ_t is a hyperparameter.

Because \mathbf{x} is unavailable during generation, we train a neural network to approximate the original data given some noisy latent and the timestep, $\hat{\mathbf{x}}_\theta(\mathbf{z}_t, t) \approx \mathbf{x}$. The denoising network can be trained utilizing a regression loss

$$L = \mathbb{E}_{\mathbf{x}, t, \mathbf{z}_t} [\|\hat{\mathbf{x}}_\theta(\mathbf{z}_t, t) - \mathbf{x}\|_2^2],$$

where $\mathbf{x} \sim p(\mathbf{x})$, $t \sim \mathcal{U}(\{1, \dots, T\})$, $\mathbf{z}_t \sim q(\mathbf{z}_t | \mathbf{x})$. We present the training procedure in Figure 1.

Given a trained denoising network, we define $p_\theta(\mathbf{z}_{t-1} | \mathbf{z}_t)$ as an approximation of the inverted forward process $q(\mathbf{z}_{t-1} | \mathbf{z}_t, \hat{\mathbf{x}}_\theta(\mathbf{z}_t, t))$, enabling us to sample from $p_\theta(\mathbf{z}_{t-1} | \mathbf{z}_t)$ in closed-form

$$\mathbf{z}_{t-1} \sim p_\theta(\mathbf{z}_{t-1} | \mathbf{z}_t) = q(\mathbf{z}_{t-1} | \mathbf{z}_t, \hat{\mathbf{x}}_\theta(\mathbf{z}_t, t)).$$

We can then draw some $\mathbf{z}_T \sim \mathcal{N}(0, 1)$ and iteratively denoise the latent by sampling $\mathbf{z}_{t-1} \sim p_\theta(\mathbf{z}_{t-1} | \mathbf{z}_t)$ until we obtain \mathbf{z}_0 , our sample from the data distribution.

For sampling from the diffusion model, we utilize the inference distribution from [Song et al. \(2020\)](#) and have

$$\begin{aligned} q(\mathbf{z}_{t-1} | \mathbf{z}_t, \mathbf{x}) = \\ \mathcal{N}(\sqrt{\alpha_{t-1}} \mathbf{x} + \sqrt{1 - \alpha_{t-1} - \sigma_t^2} \frac{\mathbf{z}_t - \sqrt{\alpha_t} \mathbf{x}}{\sqrt{1 - \alpha_t}}, \sigma_t^2 \mathbf{I}), \end{aligned} \quad (4)$$

where σ_t controls the stochasticity of the sampling procedure. Setting $\sigma_t = \sqrt{(1 - \alpha_{t-1}) / (1 - \alpha_t)} \sqrt{1 - \alpha_t / \alpha_{t-1}}$

recovers the original DDPM sampler ([Ho et al., 2020](#)) while setting $\sigma_t = 0$ gives the deterministic DDIM sampler ([Song et al., 2020](#)), both of which are evaluated in this work. We present this sampling procedure in Figure 1.

a Diffusion Training

Require: Data \mathcal{D} , Denoising Model $\hat{\mathbf{x}}_\theta()$, Timesteps T , Noise schedule α_t

- 1: **while** not converged **do** ▷ Sample data
- 2: $\mathbf{x} \sim \mathcal{D}$ ▷ Sample timestep
- 3: $t \sim \mathcal{U}(\{1, \dots, T\})$ ▷ Sample noise
- 4: $\epsilon \sim \mathcal{N}(0, \mathbf{I})$ ▷ Compute latent
- 5: $\mathbf{z}_t = \sqrt{\alpha_t} \mathbf{x} + \sqrt{1 - \alpha_t} \epsilon$ ▷ Compute loss
- 6: $L = \|\hat{\mathbf{x}}_\theta(\mathbf{z}_t, t) - \mathbf{x}\|_2^2$ ▷ Update parameters
- 7: $\theta = \theta - \eta \nabla_\theta L$ ▷ Update parameters
- 8: **end while**

b Diffusion Sampling

Require: Data \mathcal{D} , Denoising Model $\hat{\mathbf{x}}_\theta()$, Timesteps T , Noise schedule α_t , Sampling hyperparameter σ_t

- 1: $\mathbf{z}_T \in \mathbb{R}^d \sim \mathcal{N}(0, \mathbf{I})$ ▷ Sample noise
- 2: **for** $t = T, \dots, 1$ **do** ▷ Sample noise
- 3: $\epsilon \in \mathbb{R}^d \sim \mathcal{N}(0, \mathbf{I})$ ▷ Denoise latent
- 4: $\tilde{\mathbf{x}}_t = \hat{\mathbf{x}}_\theta(\mathbf{z}_t, t)$ ▷ Denoise latent
- 5: **if** $t = 1$ **then** ▷ Return generated data
- 6: **return** $\tilde{\mathbf{x}}_t$ ▷ Compute next latent
- 7: **end if**
- 8: $\tilde{\epsilon}_t = \frac{\mathbf{z}_t - \sqrt{\alpha_t} \tilde{\mathbf{x}}_t}{\sqrt{1 - \alpha_t}}$ ▷ Compute next latent
- 9: $\mathbf{z}_{t-1} = \sqrt{\alpha_{t-1}} \tilde{\mathbf{x}}_t + \sqrt{1 - \alpha_{t-1} - \sigma_t^2} \tilde{\epsilon}_t + \sigma_t \epsilon$ ▷ End for

Figure 1: Standard Diffusion Training and Sampling Algorithms

4 Methods

In this section, we lay out our approach for adapting diffusion models to language generation, termed Latent Diffusion for Language Generation (LD4LG). We first focus on the high-level modifications to the training and sampling procedures. During this discussion, we treat the denoising network, $\hat{\mathbf{x}}_\theta()$, as a black box. We discuss the exact parameterization of the network towards the end of this section.

4.1 Latent Diffusion for Language

We learn a latent diffusion model in the latent space of BART ([Lewis et al., 2020](#)), an encoder-decoder language model pre-trained as a denoising autoencoder. Given some language utterance with some tokens masked out, BART is pre-trained to generate the uncorrupted language. Unless stated otherwise, we utilize BART-base which has 6 encoder and decoder layers and a hidden size of 768. We freeze

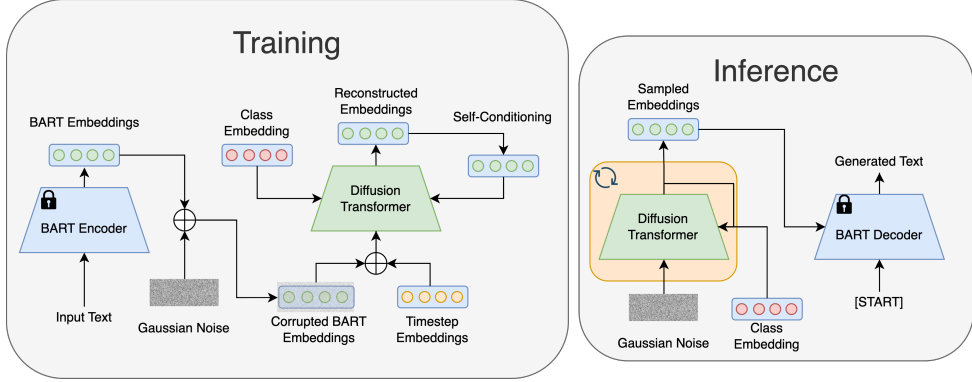


Figure 2: Overview of Latent Diffusion for Language Generation.

the BART encoder and decoder, so the only trainable parameters in our framework are those of the denoising network $\hat{\mathbf{x}}_\theta(\cdot)$.

Given some natural language which can be represented as a sequence of ℓ one-hot vectors over the vocabulary \mathcal{V} , $\mathbf{w} \in \mathbb{R}^{\ell \times |\mathcal{V}|}$, the BART encoder, $E(\cdot)$, maps it to some continuous latent space, $\mathbf{x} = E(\mathbf{w}) \in \mathbb{R}^{\ell \times d}$. The BART decoder D then approximately reconstructs the original input

$$\mathbf{w} \approx \tilde{\mathbf{w}} = D(\mathbf{x}) = D(E(\mathbf{w})) \in \mathbb{R}^{\ell \times |\mathcal{V}|}.$$

To enable training a continuous diffusion model, we therefore sample continuous data as $\mathbf{x} = E(\mathbf{w}) \in \mathbb{R}^{\ell \times d}$, $\mathbf{w} \in \mathbb{R}^{\ell \times |\mathcal{V}|} \sim \mathcal{D}$ given some dataset of natural language, \mathcal{D} . This enables training a denoising network, $\hat{\mathbf{x}}_\theta(\mathbf{z}_t, t)$, to recover \mathbf{x} .

For generation, we want to sample a latent variable, $\mathbf{z}_T \in \mathbb{R}^{\ell \times d} \sim \mathcal{N}(0, \mathbf{I})$, that is iteratively denoised to the distribution of the BART latent space. Image diffusion is typically done with a fixed resolution, $H \times W \times 3$, so it is straightforward to sample a latent variable $\mathbf{z}_T \in \mathbb{R}^{H \times W \times 3} \sim \mathcal{N}(0, \mathbf{I})$ of the appropriate shape.

Language, however, varies in length. For our data, $\mathbf{x} \in \mathbb{R}^{\ell \times d}$, ℓ varies across data samples. During training, ℓ is simply determined by the data sample. During inference, however, we must specify some ℓ_i in order to sample $\mathbf{z}_T \in \mathbb{R}^{\ell_i \times d} \sim \mathcal{N}(0, \mathbf{I})$.

To select ℓ_i at inference time, we sample ℓ_i from the empirical distribution of the lengths given by our data, $\mathcal{L}(\mathcal{D})$. In other words, we let $\Pr(\ell = \ell_i) = \frac{1}{|\mathcal{D}|} \sum_{\mathbf{w} \in \mathcal{D}} \mathbb{1}\{\mathbf{w} \in \mathbb{R}^{\ell_i \times |\mathcal{V}|}\}$. For generation, we therefore sample our latent variable by first sampling some length $\ell_i \sim \mathcal{L}(\mathcal{D})$ and then sampling the latent $\mathbf{z}_T \in \mathbb{R}^{\ell_i \times d} \sim \mathcal{N}(0, \mathbf{I})$. This enables the use of standard sampling algorithms.

4.2 Self-Conditioning

We also utilize the recently proposed self-conditioning technique introduced by Chen et al. (2022), which was found to improve sample quality. At some time t , the denoising network is typically conditioned on the latent variable and the timestep as $\tilde{\mathbf{x}}_t = \hat{\mathbf{x}}_\theta(\mathbf{z}_t, t)$. Self-conditioning proposes to additionally condition the network on its output from the previous timestep so that $\tilde{\mathbf{x}}_t = \hat{\mathbf{x}}_\theta(\mathbf{z}_t, t, \tilde{\mathbf{x}}_{t+1})$.

During inference, the sampling procedure is inherently iterative and at time t , we have already computed the output of the denoising network for the previous timestep, $\tilde{\mathbf{x}}_{t+1}$. Therefore, it does not require any additional applications of the network.

We must, however, modify the training procedure so that the denoising network learns to utilize the estimate of the data and we must define the inference behavior at time T before the first application of the denoising network.

For each training step, we sample some time $t \sim \mathcal{U}(\{1, \dots, T\})$ as before. With probability $p = 0.5$, we do not provide any estimate of the data for self-conditioning, denoted $\tilde{\mathbf{x}}_{t,\emptyset} = \hat{\mathbf{x}}_\theta(\mathbf{z}_t, t, \emptyset)$. With probability $1 - p$, however, we mimic the inference behavior by first computing $\tilde{\mathbf{x}}_{t,\emptyset} = \hat{\mathbf{x}}_\theta(\mathbf{z}_t, t, \emptyset)$ and then computing an additional estimate $\tilde{\mathbf{x}}_t = \hat{\mathbf{x}}_\theta(\mathbf{z}_t, t, \text{sg}(\tilde{\mathbf{x}}_{t,\emptyset}))$ where $\text{sg}(\cdot)$ is the stop-gradient operation. This second estimate is then used to compute the loss.

This training procedure also maintains the capacity for normal inference without self-conditioning which is utilized to generate the first estimate during sampling $\tilde{\mathbf{x}}_T = \hat{\mathbf{x}}_\theta(\mathbf{z}_T, T, \emptyset)$. Future estimates can all be computed with self-conditioning as $\tilde{\mathbf{x}}_t = \hat{\mathbf{x}}_\theta(\mathbf{z}_t, t, \tilde{\mathbf{x}}_{t+1})$.

4.3 Class-Conditional Diffusion

To evaluate the capacity of our framework for conditional language generation, we extend it to class-conditional generation. We now assume access to some dataset where each natural language utterance is associated with one of C class labels, where the class label could represent, for example, the sentiment or the topic of the text. So, we have $(\mathbf{w}, y) \in \mathcal{D}, \mathbf{w} \in \mathbb{R}^{l \times |\mathcal{V}|}, y \in \{1, 2, \dots, C\}$.

We train a class-conditional diffusion model by conditioning the denoising network on the class label during training, $\tilde{\mathbf{x}}_t = \hat{\mathbf{x}}_\theta(\mathbf{z}_t, t, y)$. Because the class label conveys information about the original data, the network will learn to utilize the additional class information to guide the denoising process. Like self conditioning, we replace the ground truth class label, y_i , with a null label, y_\emptyset , with probability $p = 0.1$ to maintain the capacity for unconditional generation.

At inference time, we can choose some class y to guide the sampling process. We sample some latent variable $\mathbf{z}_T \sim \mathcal{N}(0, \mathbf{I})$ as before and tell the denoising network that the data belongs to class y , computing $\tilde{\mathbf{x}}_t = \hat{\mathbf{x}}_\theta(\mathbf{z}_t, t, y)$ for all t . This should produce some generated text from the given class.

We provide an overview of our approach in Figure 2 and present our modified training and sampling algorithms incorporating the encoder-decoder language model, self-conditioning, and class-conditional generation in Figure 3.

4.4 Denoising Network Architecture

Our denoising network, $\tilde{\mathbf{x}}_\theta(\mathbf{z}_t, t)$, is a bidirectional Pre-LN transformer (Vaswani et al., 2017; Xiong et al., 2020) with 12 layers and a hidden dimension of $d_{\text{tx}} = 768$. We utilize learnable absolute positional encodings, T5 relative positional biases (Raffel et al., 2022), and GeGLU activations (Shazeer, 2020). The latent \mathbf{z}_t is projected to the input dimension of the transformer, passed through the transformer, and then processed with a LayerNorm (Ba et al., 2016) and a linear layer to obtain the reconstruction.

To condition on the timestep information, we adhere closely to standard practices for image diffusion and map the timestep to a sinusoidal positional encoding (denoted $\psi(t) \in \mathbb{R}^{d_{\text{tx}}}$) (Vaswani et al., 2017) which is passed through an MLP to obtain a time embedding $\text{MLP}(\psi(t)) \in \mathbb{R}^{d_{\text{tx}}}$. We add this time embedding to the input sequence and also apply adaptive layer normalization (AdaLN)

to the output of every feedforward layer, $\mathbf{h} \in \mathbb{R}^{l \times d_{\text{tx}}}$ in the encoder. Our AdaLN is defined as

$$\text{AdaLN}(\mathbf{h}, t) = \mathbf{t}_s \odot \text{LayerNorm}(\mathbf{h}) + \mathbf{t}_b,$$

where $(\mathbf{t}_s, \mathbf{t}_b) = \text{MLP}(\psi(t)) \in \mathbb{R}^{2 \times d_{\text{tx}}}$. This is implemented identically to the adaptive group normalization used for image diffusion models.

To enable self-conditioning, i.e. $\hat{\mathbf{x}}_\theta(\mathbf{z}_t, t, \tilde{\mathbf{x}}_{t+1})$, we introduce a cross-attention layer between every self-attention layer and feed-forward layer that attends to a learned projection of the previous estimate of the clean data $(\tilde{\mathbf{x}}_{t+1} \mathbf{W} + \mathbf{b}) \in \mathbb{R}^{l \times d_{\text{tx}}}$ where $\mathbf{W} \in \mathbb{R}^{d_{\text{tx}} \times d_{\text{tx}}}$, $\mathbf{b} \in \mathbb{R}^{d_{\text{tx}}}$. For denoising without the prior estimate, i.e. $\hat{\mathbf{x}}_\theta(\mathbf{z}_t, t, \emptyset)$, we cross-attend to a learnable embedding $\mathbf{h}_\theta \in \mathbb{R}^{d_{\text{tx}}}$.

To condition on some class label $y \in \{1, 2, \dots, C, \emptyset\}$, we introduce learnable class embeddings $\mathbf{C} \in \mathbb{R}^{(C+1) \times d_{\text{tx}}}$ for every class, including the null class. We condition on the class embedding with the cross-attention mechanism by concatenating the class embedding with the self-conditioning input.

4.5 Implementation Details

Image diffusion models are commonly parameterized as noise prediction models, $\hat{\epsilon}_\theta(\mathbf{z}_t, t)$, instead of as denoising models, $\hat{\mathbf{x}}_\theta(\mathbf{z}_t, t)$, although there are exceptions (Salimans and Ho, 2022). This implicitly parameterizes a denoising model

$$\hat{\mathbf{x}}_\theta(\mathbf{z}_t, t) = \frac{\mathbf{z}_t - \sqrt{1 - \alpha_t} \hat{\epsilon}_\theta(\mathbf{z}_t, t)}{\sqrt{\alpha_t}}$$

by equation (2). We found the noise prediction parameterization to be unstable and instead utilize the denoising parameterization directly.

To control the scale of the latent space, we normalize the latent space to have zero mean and unit variance and learn the diffusion model in the normalized latent space. We then undo the normalization of the space after sampling and before decoding. We compute normalization statistics from the first training batch.

We train all of our models with $T = 1000$ diffusion steps and parameterize our noise schedule, α_t , using the original linear schedule introduced by Ho et al. (2020). Sampling steps can be downsampled at inference time to accelerate generation (Song et al., 2020). We utilize 250 sampling steps with the DDPM sampler by default.

When decoding the sampled latent vectors, we utilize beam search with a beam size of 4, a repetition penalty of 1.2 (Keskar et al., 2019), and

a LD4LG Training

Require: Data \mathcal{D} , Denoising Model $\hat{\mathbf{x}}_\theta()$, Timesteps T , Noise schedule α_t
Require: Language Encoder $E()$

```
1: while not converged do
2:    $\mathbf{x} = E(\mathbf{w}), (\mathbf{w}, \mathbf{y}) \sim \mathcal{D}$   $\triangleright$  Encode sampled data
3:    $t \sim \mathcal{U}(\{1, \dots, T\})$   $\triangleright$  Sample timestep
4:    $\epsilon \sim \mathcal{N}(0, \mathbf{I})$   $\triangleright$  Sample noise
5:    $\mathbf{z}_t = \sqrt{\alpha_t} \mathbf{x} + \sqrt{1 - \alpha_t} \epsilon$   $\triangleright$  Compute latent
6:    $p \sim \mathcal{U}([0, 1])$ 
7:   if  $p < 0.1$  then
8:      $\mathbf{y} = \emptyset$   $\triangleright$  Unconditional Generation
9:   end if
10:   $\mathbf{x}_{\text{cond}} = \emptyset$   $\triangleright$  Self-conditioning
11:   $p \sim \mathcal{U}([0, 1])$ 
12:  if  $p > 0.5$  then
13:     $\mathbf{x}_{\text{cond}} = \text{sg}(\hat{\mathbf{x}}_\theta(\mathbf{z}_t, t, \emptyset, \mathbf{y}))$ 
14:  end if
15:   $L = \|\hat{\mathbf{x}}_\theta(\mathbf{z}_t, t, \mathbf{x}_{\text{cond}}, \mathbf{y}) - \mathbf{x}\|_2^2$   $\triangleright$  Compute loss
16:   $\theta = \theta - \eta \nabla_\theta L$   $\triangleright$  Update parameters
17: end while
```

b LD4LG Sampling

Require: Data \mathcal{D} , Denoising Model $\hat{\mathbf{x}}_\theta()$, Timesteps T , Noise schedule α_t , Sampling hyperparameter σ_t
Require: Language Decoder $D()$
Require: Empirical length distribution $\mathcal{L}(\mathcal{D})$
Require: Desired class label y

```
1:  $\ell_i \sim \mathcal{L}(\mathcal{D})$   $\triangleright$  Sample length
2:  $\mathbf{z}_T \in \mathbb{R}^{\ell_i \times d} \sim \mathcal{N}(0, \mathbf{I})$   $\triangleright$  Sample noise
3:  $\mathbf{x}_{\text{cond}} = \emptyset$   $\triangleright$  Self-conditioning
4: for  $t = T, \dots, 1$  do
5:    $\epsilon \in \mathbb{R}^{\ell_i \times d} \sim \mathcal{N}(0, \mathbf{I})$   $\triangleright$  Sample noise
6:    $\tilde{\mathbf{x}}_t = \hat{\mathbf{x}}_\theta(\mathbf{z}_t, t, \mathbf{x}_{\text{cond}}, \mathbf{y})$   $\triangleright$  Denoise latent
7:    $\mathbf{x}_{\text{cond}} = \tilde{\mathbf{x}}_t$   $\triangleright$  Self-conditioning
8:   if  $t = 1$  then
9:     return  $D(\tilde{\mathbf{x}}_t)$   $\triangleright$  Return decoded text
10:  end if
11:   $\tilde{\epsilon}_t = \frac{\mathbf{z}_t - \sqrt{\alpha_t} \tilde{\mathbf{x}}_t}{\sqrt{1 - \alpha_t}}$   $\triangleright$  Compute next latent
12:   $\mathbf{z}_{t-1} = \sqrt{\alpha_{t-1}} \tilde{\mathbf{x}}_t + \sqrt{1 - \alpha_{t-1} - \sigma_t^2} \tilde{\epsilon}_t + \sigma_t \epsilon$ 
13: end for
```

Figure 3: Proposed LD4LG Training and Sampling Algorithms. Deviations from the algorithms presented in Figure 1 are denoted in blue. Aspects of the algorithm unique to class-conditional diffusion are denoted in red.

prevent generations of duplicate trigrams. We provide additional details in Appendix B.

5 Datasets

E2E (Novikova et al., 2017). The E2E dataset contains a collection of 50k restaurant reviews and corresponding attributes like food type, price, location, and customer rating.

ROCStories (Mostafazadeh et al., 2016). The ROCStories dataset is a corpus of 98k five-sentence commonsense stories, that capture casual and temporal relations.

Stanford Sentiment Treebank (Socher et al., 2013). The STS dataset is a sentiment classification dataset consisting of 11,855 sentences from movie reviews.

AG News Topic Classification (Socher et al., 2013). The AG News Topic Classification dataset consists of news articles across four topics: World, Sports, Business, Sci/Tech. The dataset contains article titles and descriptions and has 120k training instances. We focus on generating the article descriptions in this work.

6 Experiments

6.1 Evaluation Metrics.

MAUVE Score (Pillutla et al., 2021) is a metric for open-ended text generation that compares the distribution of generated text with that of reference text using divergence frontiers. The divergences

are computed in a quantized embedding space and thus require an embedding model. We utilize both the GPT2-Large model (Radford et al., 2019) like Pillutla et al. (2021) and a Sentence Transformer (ST)¹ (Reimers and Gurevych, 2019).

Perplexity (Ppl) measures how likely the generated samples are according to an autoregressive language model. We use GPT2-Large to compute perplexity.

Unique Tokens (Uniq). We measure the number of unique tokens generated by the model.

Diversity (Div). We utilize the diversity metric from Su et al. (2022) and define diversity as **diversity** = $\prod_{n=2}^4 \frac{|\text{unique n-grams}(\{\mathbf{w}_i\})|}{|\text{total n-grams}(\{\mathbf{w}_i\})|}$ where $\{\mathbf{w}_i\}$ is a set of generated samples.

Memorization (Mem). The previous metrics can be optimized by generating observed samples from the training set. To quantify the degree of memorization, we measure the proportion of generated 4-grams that are found in the training set.

For all of our experiments, we sample 1000 instances from the diffusion model. For MAUVE, we sample 1000 instances from the test set to serve as the reference text. We repeat this 5 times and report the mean and standard deviation as mean_{std} . We also compute reference values for our metrics with natural samples from the test set. The reference MAUVE, for instance, is computed between 1000

¹We utilize the recommended all-mpnet-base-v2 model from <https://www.sbert.net/>.

	E2E								ROCStories							
	MAUVE \uparrow				Ppl \downarrow	Div \uparrow	Mem \downarrow	Uniq \uparrow	MAUVE \uparrow				Ppl \downarrow	Div \uparrow	Mem \downarrow	Uniq \uparrow
	GPT2		ST \uparrow						GPT2		ST					
	Train	Test	Train	Test												
Reference	.967,.006	.425,.059	.928,.009	.004,.001	117.4 _{2.7}	.020,.001	.880,.003	542 ₁₆	.959,.009	.907,.014	21.1.1	.414,.003	.364,.002	4994 ₂₇		
Diff-LM	.956,.005	.353,.021	.875,.023	.003,.000	173.7 _{6.6}	.026,.001	.871,.003	366 ₇	.043,.006	.012,.002	47.3.6	.128,.002	.434,.002	1926 ₁₇		
LD4LG	.919,.022	.395,.047	.872,.029	.005,.001	127.3 _{6.0}	.024,.002	.859,.008	403 ₁₄	.641,.036	.880,.020	31.8.3	.366,.003	.377,.004	3918 ₅₁		
GPT2	.945,.016	.450,.036	.890,.021	.005,.001	131.2 _{2.7}	.028,.001	.989,.002	523 ₂₀	.784,.012	.887,.028	19.8.2	.372,.005	.666,.007	4394.33		

Table 1: Language generation metrics for unconditional diffusion models.

	SST					AG News						
	MAUVE \uparrow		Ppl \downarrow	Div \uparrow	Mem \downarrow	Uniq \uparrow	MAUVE \uparrow		Ppl \downarrow	Div \uparrow	Mem \downarrow	Uniq \uparrow
	GPT2		ST					GPT2		ST		
	Train	Test	Train	Test	Train	Test	Train	Test	Train	Test	Train	Test
Reference	.955,.006	.925,.017	109.1 _{2.1}	.729,.004	.051,.001	4668 ₅₄	.951,.014	.911,.009	43.6 _{1.2}	.658,.002	.385,.005	7069 ₅₄
LD4LG	.626,.035	.859,.018	223.9 ₄₀	.590,.004	.095,.003	2980 ₃₁	.857,.018	.849,.032	85.3.9	.581,.003	.233,.004	5259 ₄₅
GPT2	.857,.01	.837,.033	107.8 _{4.4}	.465,.007	.957,.005	4005 ₃₉	.813,.030	.692,.052	38.0.9	.525,.014	.831,.004	6316 ₁₃₅

Table 2: Language generation metrics for class-conditional diffusion models.

train samples and 1000 test samples. We present samples from our models in Appendix D.

6.2 Unconditional Diffusion

We follow Li et al. (2022) and train unconditional diffusion models for the E2E and ROCStories datasets. We compare against their Diffusion-LM model and also fine-tune the pre-trained GPT2-Medium model, which is roughly $1.6 \times$ larger than our diffusion model. For sampling from GPT2, we prompt it with a BOS token and utilize nucleus sampling ($p = 0.95$) (Holtzman et al., 2020).

We report results for these experiments in Table 1. We utilize the E2E dataset to enable direct comparison with the prior Diffusion-LM model, but its curation complicates evaluation. It is split so that reviews with similar characteristics are constrained within a single split which introduces a distribution shift between splits. To observe this, we compute MAUVE scores for training and test instances. The reference MAUVE scores show that training reviews are distributed similarly, but training and test reviews are from different distributions.

We observe that LD4LG does achieve a higher test MAUVE than Diffusion-LM, but the variance is reasonably high and the reference metrics show that the E2E dataset is very repetitive, with limited diversity and a small vocabulary.

As a result, the more complex ROCStories is more informative. We observe that LD4LG is more effective than Diffusion-LM at modeling complex language, achieving higher MAUVE scores with lower perplexity, greater diversity, and less memorization. This highlights the benefit of using a high quality latent space from a language model rather

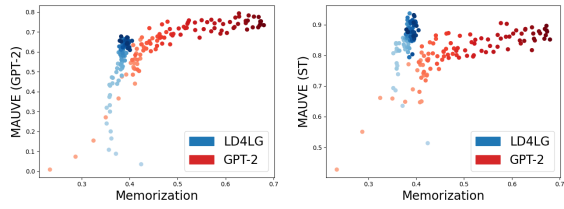


Figure 4: Trade-off between MAUVE scores and memorization for ROCStories. Darker points occurred later in training.

than learning the representation space from scratch.

GPT2 generally achieves strong language metrics, but appears to be more susceptible to memorization. To quantify the trade-off between memorization and the MAUVE scores, we plot the memorization and validation MAUVE scores over the course of training for the two models in Figure 4. For a given level of memorization, LD4LG achieves a higher MAUVE score than the GPT2 model, demonstrating that LD4LG is better-suited for sampling novel language from the distribution.

We do find the GPT2 samples have lower perplexity. However, measuring perplexity with a pre-trained GPT2 model may bias the metric towards the fine-tuned GPT2 model, and MAUVE scores have a stronger correlation with human judgements of quality (Pillutla et al., 2021).

6.3 Class-Conditional Diffusion

We train the class-conditional diffusion models for the SST and AG News datasets. We first verify that our training procedure maintains the capacity for high-quality unconditional generation by comparing our models against fine-tuned GPT2 models.

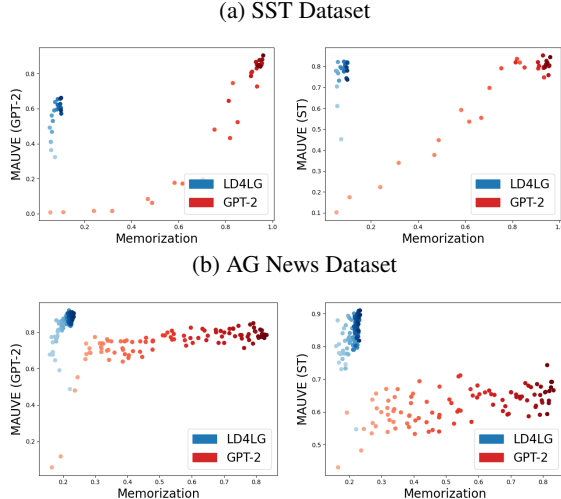


Figure 5: Trade-off between MAUVE scores and memorization for SST and AG News datasets. Darker points occurred later in training.

We report the language generation metrics in Table 2 and plot the trade-off between MAUVE scores and memorization in Figure 5. The diffusion models still achieve strong MAUVE scores, although their perplexity again lags behind GPT2. We observe that the diffusion model is somewhat susceptible to memorization for the smallest dataset, SST, and it occasionally reproduces short instances from the training set. However, GPT2 is even more susceptible to memorization for these datasets.

6.3.1 Conditional Generation

We sample instances for each class and compute the MAUVE scores between the samples and natural instances from each class. These metrics are reported in Table 3. We observe that the MAUVE scores are consistently highest when the conditioning and ground-truth labels are aligned, demonstrating that the label guides the generation effectively.

We also perform an additional experiment to measure the quality of the generated data. We sample 1000 instances evenly distributed among the classes. We then train a classification model with the synthetic text and evaluate its performance on heldout data. We compare against a classifier trained with 1000 instances from the training set.

We report the results from fine-tuning DeBERTa-v3-base (He et al., 2021) in Table 4. The synthetic data provides a strong training signal to the classification model, enabling it to generalize effectively to natural language data. This further demonstrates the efficacy of class-conditioning.

SST				
Conditioning	MAUVE \uparrow			
	GPT2		ST	
	Positive	Negative	Positive	Negative
Positive	.600. _{.034}	.224. _{.010}	.789. _{.044}	.119. _{.015}
Negative	.220. _{.016}	.585. _{.013}	.116. _{.014}	.803. _{.038}

AG News				
Conditioning	MAUVE (GPT2) \uparrow			
	World	Sports	Business	Sci/Tech
	.852. _{.016}	.019. _{.001}	.038. _{.003}	.029. _{.006}
World	.803. _{.022}	.000. _{.000}	.002. _{.001}	.001. _{.000}
Sports	.001. _{.000}	.880. _{.025}	.000. _{.000}	.000. _{.000}
Business	.003. _{.000}	.000. _{.000}	.767. _{.034}	.011. _{.001}
Sci/Tech	.002. _{.000}	.000. _{.000}	.012. _{.001}	.852. _{.038}

Table 3: Metrics for class-conditional generation.

Training Data	SST		AG News	
	Accuracy			
Natural (1000 samples)	.885. _{.005}		.889. _{.002}	
Synthetic (1000 samples)	.860. _{.010}		.866. _{.006}	

Table 4: Classifier performance.

ROCStories	ROCStories				
	MAUVE \uparrow		Ppl \downarrow	Div \uparrow	Mem \downarrow
	GPT2	ST			
LD4LG	.641. _{.036}	.880. _{.020}	31.8. _{.3}	.366. _{.003}	.377. _{.004}
- Self-cond.	.477. _{.028}	.869. _{.026}	52.2. _{.8}	.357. _{.002}	.344. _{.003}
					3918 _{.51}
					4027 _{.51}

Table 5: Impact of Self-conditioning

6.4 Ablation Studies

We ablate the impact of self-conditioning in Table 5. We find that self-conditioning significantly improves the MAUVE scores and the perplexity of generated text, but it does slightly increase the memorization.

We ablate other design decisions such as the effect of different sampling configurations, the effect of scaling the denoising network, and the impact of using BART-large instead of BART-base. We present these results in Appendix A.

7 Conclusion

In this work, we demonstrate that continuous diffusion models can be learned in the latent space

of a pre-trained encoder-decoder language model. We can then sample continuous latent vectors and decode them into natural language with the pre-trained decoder.

This approach augments the generative capability of the pre-trained language model and enables high quality unconditional language generation from a specified data distribution. We further extend our framework to class-conditional generation and demonstrate that our approach enables conditional language generation.

Acknowledgements

This research is supported by grants from the National Science Foundation NSF (IIS-2107161, III-1526012, IIS-1149882, and IIS-1724282), the Cornell Center for Materials Research with funding from the NSF MRSEC program (DMR-1719875), and DARPA.

References

Jacob Austin, Daniel D. Johnson, Jonathan Ho, Daniel Tarlow, and Rianne van den Berg. 2021. [Structured denoising diffusion models in discrete state-spaces](#). In *Advances in Neural Information Processing Systems*.

Jimmy Ba, Jamie Ryan Kiros, and Geoffrey E. Hinton. 2016. Layer normalization. *ArXiv*, abs/1607.06450.

Tom Brown, Benjamin Mann, Nick Ryder, Melanie Subbiah, Jared D Kaplan, Prafulla Dhariwal, Arvind Neelakantan, Pranav Shyam, Girish Sastry, Amanda Askell, Sandhini Agarwal, Ariel Herbert-Voss, Gretchen Krueger, Tom Henighan, Rewon Child, Aditya Ramesh, Daniel Ziegler, Jeffrey Wu, Clemens Winter, Chris Hesse, Mark Chen, Eric Sigler, Mateusz Litwin, Scott Gray, Benjamin Chess, Jack Clark, Christopher Berner, Sam McCandlish, Alec Radford, Ilya Sutskever, and Dario Amodei. 2020. [Language models are few-shot learners](#). In *Advances in Neural Information Processing Systems*, volume 33, pages 1877–1901. Curran Associates, Inc.

Ting Chen, Ruixiang Zhang, and Geoffrey Hinton. 2022. Analog bits: Generating discrete data using diffusion models with self-conditioning. *arXiv preprint arXiv:2208.04202*.

J. Choi, J. Lee, C. Shin, S. Kim, H. Kim, and S. Yoon. 2022. [Perception prioritized training of diffusion models](#). In *2022 IEEE/CVF Conference on Computer Vision and Pattern Recognition (CVPR)*, pages 11462–11471, Los Alamitos, CA, USA. IEEE Computer Society.

Aakanksha Chowdhery, Sharan Narang, Jacob Devlin, Maarten Bosma, Gaurav Mishra, Adam Roberts, Paul Barham, Hyung Won Chung, Charles Sutton, Sebastian Gehrmann, et al. 2022. [Palm: Scaling language modeling with pathways](#). *arXiv preprint arXiv:2204.02311*.

Prafulla Dhariwal and Alexander Nichol. 2021. [Diffusion models beat gans on image synthesis](#). In *Advances in Neural Information Processing Systems*, volume 34, pages 8780–8794. Curran Associates, Inc.

Ian Goodfellow, Jean Pouget-Abadie, Mehdi Mirza, Bing Xu, David Warde-Farley, Sherjil Ozair, Aaron Courville, and Yoshua Bengio. 2014. [Generative adversarial nets](#). In *Advances in Neural Information Processing Systems*, volume 27. Curran Associates, Inc.

Pengcheng He, Jianfeng Gao, and Weizhu Chen. 2021. [Debertav3: Improving deberta using electra-style pre-training with gradient-disentangled embedding sharing](#).

Jonathan Ho, William Chan, Chitwan Saharia, Jay Whang, Ruiqi Gao, Alexey Gritsenko, Diederik P Kingma, Ben Poole, Mohammad Norouzi, David J Fleet, et al. 2022. [Imagen video: High definition video generation with diffusion models](#). *arXiv preprint arXiv:2210.02303*.

Jonathan Ho, Ajay Jain, and Pieter Abbeel. 2020. [Denoising diffusion probabilistic models](#). *CoRR*, abs/2006.11239.

Ari Holtzman, Jan Buys, Li Du, Maxwell Forbes, and Yejin Choi. 2020. [The curious case of neural text degeneration](#). In *International Conference on Learning Representations*.

Emiel Hoogeboom, Didrik Nielsen, Priyank Jaini, Patrick Forré, and Max Welling. 2021. [Argmax flows and multinomial diffusion: Learning categorical distributions](#). *Advances in Neural Information Processing Systems*, 34:12454–12465.

Nitish Shirish Keskar, Bryan McCann, Lav R Varshney, Caiming Xiong, and Richard Socher. 2019. [Ctrl: A conditional transformer language model for controllable generation](#). *arXiv preprint arXiv:1909.05858*.

Zhifeng Kong, Wei Ping, Jiaji Huang, Kexin Zhao, and Bryan Catanzaro. 2021. [Diffwave: A versatile diffusion model for audio synthesis](#). In *International Conference on Learning Representations*.

Mike Lewis, Yinhan Liu, Naman Goyal, Marjan Ghazvininejad, Abdelrahman Mohamed, Omer Levy, Veselin Stoyanov, and Luke Zettlemoyer. 2020. [BART: Denoising sequence-to-sequence pre-training for natural language generation, translation, and comprehension](#). In *Proceedings of the 58th Annual Meeting of the Association for Computational Linguistics*, pages 7871–7880, Online. Association for Computational Linguistics.

Xiang Lisa Li, John Thickstun, Ishaan Gulrajani, Percy Liang, and Tatsunori B. Hashimoto. 2022. [Diffusion-lm improves controllable text generation](#).

Ilya Loshchilov and Frank Hutter. 2019. [Decoupled weight decay regularization](#). In *International Conference on Learning Representations*.

Nasrin Mostafazadeh, Nathanael Chambers, Xiaodong He, Devi Parikh, Dhruv Batra, Lucy Vanderwende, Pushmeet Kohli, and James Allen. 2016. A corpus and cloze evaluation for deeper understanding of commonsense stories. In *Proceedings of the 2016 Conference of the North American Chapter of the Association for Computational Linguistics: Human Language Technologies*, pages 839–849.

Alexander Quinn Nichol and Prafulla Dhariwal. 2021. [Improved denoising diffusion probabilistic models](#). In *Proceedings of the 38th International Conference on Machine Learning*, volume 139 of *Proceedings of Machine Learning Research*, pages 8162–8171. PMLR.

Jekaterina Novikova, Ondřej Dušek, and Verena Rieser. 2017. The e2e dataset: New challenges for end-to-end generation. *arXiv preprint arXiv:1706.09254*.

Ethan Perez, Douwe Kiela, and Kyunghyun Cho. 2021. [True few-shot learning with language models](#). In *Advances in Neural Information Processing Systems*.

Krishna Pillutla, Swabha Swayamdipta, Rowan Zellers, John Thickstun, Sean Welleck, Yejin Choi, and Zaid Harchaoui. 2021. Mauve: Measuring the gap between neural text and human text using divergence frontiers. *Advances in Neural Information Processing Systems*, 34:4816–4828.

Alec Radford, Jeff Wu, Rewon Child, David Luan, Dario Amodei, and Ilya Sutskever. 2019. Language models are unsupervised multitask learners.

Colin Raffel, Noam Shazeer, Adam Roberts, Katherine Lee, Sharan Narang, Michael Matena, Yanqi Zhou, Wei Li, and Peter J. Liu. 2022. Exploring the limits of transfer learning with a unified text-to-text transformer. *J. Mach. Learn. Res.*, 21(1).

Aditya Ramesh, Prafulla Dhariwal, Alex Nichol, Casey Chu, and Mark Chen. 2022. Hierarchical text-conditional image generation with clip latents. *arXiv preprint arXiv:2204.06125*.

Nils Reimers and Iryna Gurevych. 2019. [Sentence-bert: Sentence embeddings using siamese bert-networks](#). In *Proceedings of the 2019 Conference on Empirical Methods in Natural Language Processing*. Association for Computational Linguistics.

Robin Rombach, Andreas Blattmann, Dominik Lorenz, Patrick Esser, and Björn Ommer. 2022. High-resolution image synthesis with latent diffusion models. In *Proceedings of the IEEE/CVF Conference on Computer Vision and Pattern Recognition (CVPR)*, pages 10684–10695.

Chitwan Saharia, William Chan, Saurabh Saxena, Lala Li, Jay Whang, Emily Denton, Seyed Kamalar Seyed Ghasemipour, Raphael Gontijo-Lopes, Burcu Karagol Ayan, Tim Salimans, Jonathan Ho, David J. Fleet, and Mohammad Norouzi. 2022. [Photorealistic text-to-image diffusion models with deep language understanding](#). In *Advances in Neural Information Processing Systems*.

Tim Salimans and Jonathan Ho. 2022. [Progressive distillation for fast sampling of diffusion models](#). In *International Conference on Learning Representations*.

Noam Shazeer. 2020. Glu variants improve transformer. *arXiv preprint arXiv:2002.05202*.

Richard Socher, Alex Perelygin, Jean Wu, Jason Chuang, Christopher D Manning, Andrew Y Ng, and Christopher Potts. 2013. Recursive deep models for semantic compositionality over a sentiment treebank. In *Proceedings of the 2013 conference on empirical methods in natural language processing*, pages 1631–1642.

Jascha Sohl-Dickstein, Eric A. Weiss, Niru Maheswaranathan, and Surya Ganguli. 2015. [Deep unsupervised learning using nonequilibrium thermodynamics](#).

Jiaming Song, Chenlin Meng, and Stefano Ermon. 2020. [Denoising diffusion implicit models](#). *CoRR*, abs/2010.02502.

Robin Strudel, Corentin Tallec, Florent Altché, Yilun Du, Yaroslav Ganin, Arthur Mensch, Will Grathwohl, Nikolay Savinov, Sander Dieleman, Laurent Sifre, and Rémi Leblond. 2022. [Self-conditioned embedding diffusion for text generation](#).

Yixuan Su, Tian Lan, Yan Wang, Dani Yogatama, Lingpeng Kong, and Nigel Collier. 2022. A contrastive framework for neural text generation. *arXiv preprint arXiv:2202.06417*.

Ashish Vaswani, Noam Shazeer, Niki Parmar, Jakob Uszkoreit, Llion Jones, Aidan N. Gomez, Łukasz Kaiser, and Illia Polosukhin. 2017. Attention is all you need. In *Proceedings of the 31st International Conference on Neural Information Processing Systems, NIPS’17*, page 6000–6010, Red Hook, NY, USA. Curran Associates Inc.

Ruixin Xiong, Yunchang Yang, Di He, Kai Zheng, Shuxin Zheng, Chen Xing, Huishuai Zhang, Yanyan Lan, Liwei Wang, and Tieyan Liu. 2020. [On layer normalization in the transformer architecture](#). In *Proceedings of the 37th International Conference on Machine Learning*, volume 119 of *Proceedings of Machine Learning Research*, pages 10524–10533. PMLR.

A Ablations

We present the results from different sampling configurations for the ROCStories dataset in Table 6. We also report the wall clock time needed to generate the 1000 samples across the different numbers of sampling timesteps while batching the generations with a batch size of 64. A major drawback of our approach is that sampling from diffusion models is time-intensive due to the iterative nature of the generative process. However, speeding up sampling is an active area of research and many techniques developed for image diffusion models (e.g. progressive distillation (Salimans and Ho, 2022)) could likely be adapted to speed up sampling for our framework as well.

We find that the number of sampling steps introduces a tradeoff between the diversity and the quality of the text, with more sampling steps leading to more fluent but less diverse text and fewer sampling steps leading to less fluent but more diverse text. The MAUVE metrics are maximized when utilizing only 250 steps, demonstrating that our chosen sampling configuration achieves a reasonable balance between diversity and quality. We also find that the DDPM sampler is generally more effective than the DDIM sampler, except when using very few time steps.

We ablate additional aspects of our proposed framework by training unconditional diffusion models on the ROCStories dataset. We examine the impact of scaling up the denoising network in Table 7. We observe that the performance of the model scales favorably with the size of the denoising network, suggesting that further performance improvements can likely be gained by further scaling up the denoising network.

We also ablate the decisions related to training the diffusion model. We report the effect of utilizing a cosine noise schedule (Nichol and Dhariwal, 2021) or different loss functions in Table 8. We observe that the different training configurations have disparate impacts across different language generation metrics. While our default configuration achieves the highest MAUVE (GPT2) score and the lowest perplexity, utilizing either a cosine schedule or the L2 loss improves the diversity of generations and the L2 loss improves the MAUVE (ST) score. After the introduction of DDPM for image synthesis, multiple improved noise schedules have been introduced (Nichol and Dhariwal, 2021; Choi et al., 2022). Similar optimizations can likely

be made for language generation.

We also examine the impact of using BART-large instead of BART-base as our language model in Table 9. We find, perhaps surprisingly, that utilizing BART-large generally degrades performance, with the exception of perplexity which benefits from the larger language model. Utilizing BART-large does increase the dimensionality of the latent space. Learning effective diffusion models in that latent space may therefore require larger volumes of data or higher-capacity denoising networks. Scaling diffusion models to the latent spaces of larger language models is an important direction for future work.

B Implementation Details

All of the models presented in this work are trained on either a single Nvidia A6000 or a single Nvidia 3090.

B.1 Latent Diffusion For Language Generation

We present the training details across the different datasets in Table 10. We used the same hyperparameters across datasets, except that we increased the strength of the regularization for the simplest two datasets, E2E and SST. We also found that training for longer was beneficial for the larger, more complex datasets.

We also report the wall clock times for training the models, although our implementation is not optimized for runtime. The primary cause of the slowdown for AG News compared to ROCStories, for instance, stems from additional validation sampling and logging for class-conditional generation during training.

When normalizing the latent space, we utilize the first batch of training data to compute the mean for each feature dimension, averaging across the samples in the batch and the sequence lengths of the samples. Therefore, we compute the mean vector $\hat{\mu} = \frac{1}{b\ell} \sum_{b,\ell} \mathbf{x}_{b,\ell}$, $\hat{\mu} \in \mathbb{R}^d$ where $\mathbf{x} \in \mathbb{R}^{b \times \ell \times d}$ is some batched data. We then compute the global variance across all dimensions in the centered latent space $\hat{\sigma}^2 = \frac{1}{b\ell d} \sum_{b,\ell,d} (\mathbf{x}_{b,\ell,d} - \hat{\mu}_d)^2$, $\hat{\sigma}^2 \in \mathbb{R}$ to rescale the latent space to have unit variance.

B.2 Diffusion LM

We train our Diffusion-LM models utilizing the public implementation by Li et al. (2022)² and the

²<https://github.com/XiangLi1999/Diffusion-LM>

ROCStories								
Sampling Steps	Sampler	MAUVE \uparrow		Ppl \downarrow	Div \uparrow	Mem \downarrow	Uniq \uparrow	Wall Clock Time (1000 samples)
		GPT2	ST					
50	DDIM	.521 _{.033}	.878 _{.032}	52.8 _{.7}	.414 _{.002}	.303 _{.004}	4552 _{.52}	2m17s
	DDPM	.489 _{.029}	.799 _{.044}	54.7 _{.7}	.443 _{.003}	.276 _{.002}	4823 _{.52}	
100	DDIM	.602 _{.014}	.901 _{.018}	42.5 _{.3}	.390 _{.002}	.338 _{.003}	4253 _{.45}	3 m33s
	DDPM	.597 _{.037}	.900 _{.022}	41.7 _{.3}	.405 _{.003}	.328 _{.002}	4316 _{.38}	
250	DDIM	.610 _{.035}	.911 _{.008}	35.1 _{.5}	.364 _{.005}	.372 _{.004}	4004 _{.53}	7m18s
	DDPM	.641 _{.036}	.880 _{.020}	31.8 _{.3}	.366 _{.003}	.377 _{.004}	3918 _{.51}	
500	DDIM	.631 _{.022}	.876 _{.035}	32.1 _{.5}	.351 _{.004}	.388 _{.003}	3895 _{.44}	14m6s
	DDPM	.629 _{.025}	.869 _{.031}	28.4 _{.5}	.348 _{.004}	.397 _{.004}	3750 _{.36}	
1000	DDIM	.600 _{.023}	.862 _{.036}	30.4 _{.1}	.342 _{.002}	.398 _{.003}	3825 _{.29}	26m1s
	DDPM	.625 _{.023}	.852 _{.015}	26.7 _{.4}	.335 _{.002}	.410 _{.003}	3628 _{.38}	

Table 6: Evaluation of different sampling configurations. We use 250 steps with the DDPM sampler by default.

ROCStories									
	Num Layers	Hidden Dim	Trainable Params	MAUVE \uparrow		Ppl \downarrow	Div \uparrow	Mem \downarrow	Uniq \uparrow
				GPT2	ST				
LD4LG	8	512	66M	.560 _{.038}	.845 _{.024}	32.1 _{.3}	.322 _{.003}	.396 _{.002}	3332 _{.44}
	12	768	214M	.641 _{.036}	.880 _{.020}	31.8 _{.3}	.366 _{.003}	.377 _{.004}	3918 _{.51}
	16	1024	498M	.667 _{.027}	.879 _{.009}	29.4 _{.5}	.371 _{.004}	.390 _{.004}	4226 _{.38}

Table 7: Effect of scaling the denoising network. Our default configuration uses 12 layers and a hidden dimension of 768.

ROCStories								
	Noise Schedule	Loss	MAUVE \uparrow		Ppl \downarrow	Div \uparrow	Mem \downarrow	Uniq \uparrow
			GPT2	ST				
LD4LG	Linear	L1	.641 _{.036}	.880 _{.020}	31.8 _{.3}	.366 _{.003}	.377 _{.004}	3918 _{.51}
	Cosine	L1	.632 _{.037}	.885 _{.029}	47.1 _{.2}	.414 _{.004}	.311 _{.003}	4334 _{.19}
	Linear	L2	.606 _{.032}	.914 _{.014}	32.9 _{.2}	.390 _{.002}	.359 _{.002}	4186 _{.43}

Table 8: Ablation of diffusion training configuration. Our default configuration uses a linear schedule with the L1 loss.

ROCStories							
	Language Model	MAUVE \uparrow		Ppl \downarrow	Div \uparrow	Mem \downarrow	Uniq \uparrow
		GPT2	ST				
LD4LG	BART-base	.641 _{.036}	.880 _{.020}	31.8 _{.3}	.366 _{.003}	.377 _{.004}	3918 _{.51}
	BART-large	.425 _{.025}	.863 _{.014}	29.0 _{.4}	.348 _{.002}	.390 _{.003}	3917 _{.42}

Table 9: Ablation of language model. We use BART-base by default.

provided commands for the E2E and ROCStories datasets.

B.3 GPT2

We present the default hyperparameters for the GPT2-Medium baseline in Table 11. We additionally perform a grid search over learning rate values in $[2e-5, 5e-5, 8e-5]$ and visualize these results in Figure 6. We observe that our findings with respect to memorization are consistent across hyperparameters. For sampling from GPT2, we prompt it with a BOS token and utilize nucleus sampling ($p = 0.95$). We use the same repetition penalty of 1.2 (Keskar et al., 2019) that we use for the BART decoder and similarly prevent generations of duplicate trigrams.

B.4 Classifier

We present the hyperparameters for the classifier in Table 12. We use the same hyperparameters across all classification experiments.

B.5 Evaluation Metrics

For the MAUVE score, we utilize the default parameters when utilizing GPT2-Large. When utilizing the sentence transformer, we observed some issues with the score saturating, so we increased the scaling factor to $c = 8$ following advice from the official implementation (<https://github.com/krishnap25/mauve>). Increasing the scaling factor increases the variance of the score, but we report the standard deviation across all experiments to quantify that variance.

For the n-gram metrics, we utilize the `en_core_web_sm` tokenizer from Spacy (<https://spacy.io/>) to split the generations into tokens.

C Dataset Statistics

E2E (Novikova et al., 2017). We utilize the same training, validation, and testing splits as Li et al. (2022). This leaves us with 42,061 training instances, 4,672 validation instances, and 4,693 test instances.

ROCStories (Mostafazadeh et al., 2016). The dataset consists of 98,161 instances. We hold out 1,000 instances for validation, 4,000 instances for testing, and utilize the remaining 93,161 instances for training.

Stanford Sentiment Treebank (Socher et al., 2013). We binarize the continuous sentence-level labels to produce a binary classification dataset and follow the official train/validation/testing splits.

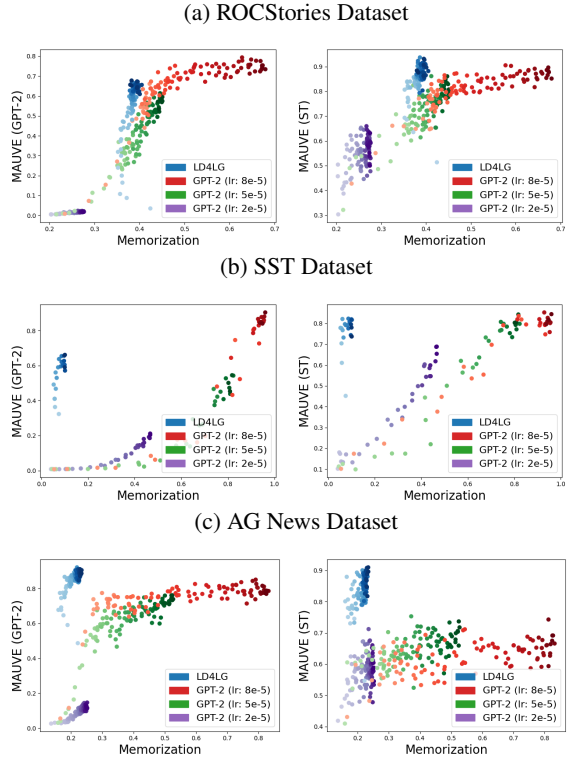


Figure 6: Trade-off between MAUVE scores and memorization for LD4LG and GPT2 with different learning rates. Darker points occurred later in training.

This leaves us with 8,544 training instances, 1,101 validation instances, and 2,210 test instances.

AG News Topic Classification (Socher et al., 2013). The dataset consists of titles and short descriptions from news articles. We discard the titles and focus on generating the descriptions in this work. The official train/test splits have 120k training instances and 7,600 testing instances. We hold out 1,000 instances from the training set for validation. We therefore utilize 119k training instances, 1,000 validation instances, and 7,600 test instances.

D Qualitative Examples

We present random unconditional samples from the diffusion models for ROCStories (Table 13), E2E (Table 14), SST (Table 15), and AG News (Table 16). For each random sample, we utilize the sentence transformer to retrieve and display the most similar training instance to examine whether memorization is occurring.

For the E2E dataset, which consists of many similar reviews, we present the top two examples to illustrate the repetitive nature of the dataset.

We also present conditional generations for the SST (Table 17) and AG News datasets (Table 18)

	E2E	ROCStories	SST	AG News
Model		LD4LG		
Trainable Params		214M		
Max Seq Length		64		
Diffusion Steps		1000		
Noise Schedule		Linear		
Regression Loss		L1		
Transformer Layers		12		
Transformer Dimension		768		
Optimizer	AdamW (Loshchilov and Hutter, 2019)			
Learning Rate		1e-4		
(β_1, β_2)		(0.9, 0.999)		
Batch Size		64		
Warmup Steps		1000		
Learning Rate Schedule		Cosine Decay		
Weight Decay	1e-2	1e-6	1e-2	1e-6
Dropout	0.1	0.0	0.1	0.0
Gradient Clipping		1.0		
EMA Decay		0.9999		
Iterations	100k	500k	100k	500k
Training Time	15h 53m	3d 12h 43m	22h 43m	4d 13h 13m

Table 10: Training details for our framework across different datasets.

	E2E	ROCStories	SST	AG News
Model		GPT2-Medium		
Trainable Params		355M		
Max Seq Length		64		
Optimizer	AdamW (Loshchilov and Hutter, 2019)			
Learning Rate		8e-5		
(β_1, β_2)		(0.9, 0.999)		
Batch Size		32		
Warmup Steps		500		
Learning Rate Schedule		Linear Decay		
Weight Decay		1e-2		
Dropout		0.1		
Gradient Clipping		1.0		
Iterations	50k	100k	30k	100k

Table 11: Training details for our autoregressive baseline across different datasets.

	SST	AG News
Model		DeBERTa-v3-base
Trainable Params		184M
Max Seq Length		64
Optimizer	AdamW (Loshchilov and Hutter, 2019)	
Learning Rate		2e-5
(β_1, β_2)		(0.9, 0.999)
Batch Size		32
Warmup Steps		100
Learning Rate Schedule		Linear Decay
Weight Decay		1e-2
Dropout		0.1
Gradient Clipping		1.0
Iterations		3k

Table 12: Training details for our classification model.

for all of the classes.

Unconditional LD4LG Sample	Closest Training Instance
Kelley went to the attic. There was a ladder on the roof. Kelley we you jumped off the ladder. She landed on her shoulder. She twisted her hip.	Alicia was playing in the treehouse. To her dismay however she fell from the top. She was on the ladder when she fell. When she fell she broke her wrist. Alicia had to get a cast.
Ann hated cleaning her bed. She always wanted it being rinsed. She hired a maid. The maid made her bed very well ruffed. Ann admired her maid too.	John hated to do his own laundry. He could never figure it out. He hired a maid to do it for him. The maid did an excellent job. He never had to do laundry again.
Gary is a horrible employee. I work full time every day. I have to work for 8 days a week. I hate the kids. My kids like the babysitters so I don't hate them.	Timmy works as a manager for the Dollar Tree. He's paid salary, but his contract states he has to work 45 hours. His district manager will reprimand him if he doesn't work 52 hours. The discrepancy in hours worked means he's paid less than assistants. Because of this, he's looking for a new job.
Stacy was in a bad mood. Her parents were putting her in detention. Today was a tough day. Stacy didn't seem to change her mood. Stacy was locked out.	Drew was weak from his medications. He didn't go to school today. A friend called him at night to see if he was okay. He said that school was beyond fun today. Drew found out that there was a large assembly and party there.
I gave my brother-law a Jack Jack box to my wife. She didn't mean to keep it for romantic feelings. She tried to hide it on her way to work. I eventually returned the box to another coworker. She was heartbroken.	I handed my gift to my sister. She quickly opened it to see what's inside. The gift was something that she requested for weeks. However, she had a mean grin since she changed her mind about it. I took the gift back and walked away.
Ben was a very depressed man. His depression and his mind was failing. Ben decided to go to therapy daily. After going to the therapy, Ben noticed his attitude had gone up. He suddenly felt more confident about the future and future in life.	Kevin was feeling upset lately. His parents started him in therapy. At first Kevin was reluctant to speak to his therapist. But when they started speaking, he felt better. Slowly Kevin let the therapist improve his mental health.
Bill was adventurous, and loved to go rock- diving. A buddy Jim made a bet on him to go up a tall cliff. He had it it, and started way up up the top. But when he bent down to rest his breath, he felt a pain. He was scared, but	Bill was an expert climber. He had trained his whole life for one reason. He wanted to climb the world's tallest mountain. Despite his training, he was unable to make it to the top. Bill lost his grip, and he fell down the mountain.
Megan's credit debt reached her 6 months. She tried to turn in the payment but she had \$12,000 dollars due. She had \$500 dollars due but she tried the bank to find a way to get her money paid. Finally, to try to cover her credit debt she tried to get	Matt has a bad relationship with his mother. His mother used his credit card and took out 5000 worth of loans Matt now owes \$5000 but he won't sue his mom Luckily, he had enough money to pay it back Everything ended up okay
ShShShakla took a walk through the park. It was quiet and quiet. She walked in a quiet part of the park, She then watched a sports movie. She then went home.	Irina wanted to enjoy the outdoors. She went to the park and took a long walk. An hour later, she was exhausted. It had been great to spend the day enjoying nature. Irina decided to come back the next day as well.

Table 13: Random samples from ROCStories dataset.

Unconditional LD4LG Sample	Closest Training Instance	Second Closest Training Instance
The high priced children friendly Italian restaurant Blue Spice in riverside.	The high priced restaurant, Blue Spice, is located in riverside. It is children friendly and is highly rated	An expensive fast food restaurant in Riverside called 'Blue Spice'.
Aromi is an English restaurant situated by the riverside.	Aromi is a restaurant in the riverside area which serves English food.	The Aromi is a restaurant located near the riverside. It serves English food.
Low rated low rated coffee shop for children's city centre are not allowed	There is a coffee shop Aromi located in City Centre that is not family friendly.	There is an average rated Italian coffee shop with a high price range located in the city centre area named Fitzbillies that is not child friendly
The 3 star restaurant, The Cambridge Blue, offers great meals.	The Cambridge Blue is a traditionally British restaurant, offering 3 star food	The Cambridge Blue is a 3 star restaurant that offers a selection of wine, spirits and appetizers.
The Punter is located near of The Portland Arms in City centre. It has moderate prices food and is kid friendly.	The Punter is a kids friendly place in the city centre near The Portland Arms. It has a moderate price range.	The Punter is a restaurant in city centre near The Portland Arms. They offer a kid friendly environment with a moderately priced menu.
The Phoenix restaurant serves French food and is located in the riverside area. Customer rating 3 out of 5 stars.	The Phoenix serves French food and is located in the riverside area. It has an average customer rating of 1 out of 5.	The Phoenix offers French food and has a customer rating of 5 out of 5. It is located in the riverside.
Browns Cambridge is a coffee shop that has a customer rating of 3 out of 5. They serve French food. It is in Riverside near the Crowne Plaza Hotel and is child friendly.	Browns Cambridge is a coffee shop with French food. It has a 1 - 5 customer rating, and is kid friendly. It is in the area of riverside and near Crown Plaza Hotel.	Browns Cambridge is a coffee shop with a customer rating of 5 out of 5 serving French food. It is near the Crowne Plaza Hotel on the riverside.
Blue Spice coffee shop is riverside near Avalon. Yes, the customer ratings are average but the prices are little high but it's by the riverside and its kids are welcome.	Blue Spice is a coffee shop that is in the riverside area near Avalon that gets great customer ratings, is priced moderately, but is not very kid friendly.	Blue Spice coffee shop rated 1 out of 5, kid friendly, moderate prices near Avalon in riverside.
The Wildwood is a high priced Italian pub with an average customer rating	The Italian pub Wildwood gets average ratings from customers with prices ranging in the high side.	High priced English pub Wildwood has an average customer rating.

Table 14: Random samples from E2E dataset.

Unconditional LD4LG Sample	Closest Training Instance
Silly, loud and goofy.	Silly, loud and goofy.
A riveting story of friendship.	A riveting story well told.
A colorful, colorful, vibrant, colorful yarn.	By-the-numbers yarn.
This is not original writing.	It's not original enough.
If you're looking for a film full of its problems, you should't see again again.	It's an ambitious film, and as with all ambitious films, it has some problems.
A 90-minute movie with middling performances, some awkward dialogue and a m m middling ending.	A movie that's held captive by mediocrity.
(Elsa/Getty Images) makes a good nomination for an Oscar Oscar, but she doesn't quite earn an Oscar nomination she obviously deserves an Oscar award. Oscar Oscar Oscar nomination.	Forget about one Oscar nomination for Julianne Moore this year - she should get all five.
The film's plot is a bit contrived – or even a few of visual delights – with the contrived humor that Fosters, but it never lets go of its contrived and absurd plot twists.	Beneath the uncanny, inevitable and seemingly shrewd facade of movie-biz farce... lies a plot cobbled together from largely flat and uncreative moments.
Smaller kids will be disappointed.	Smaller numbered kidlets will enjoy.

Table 15: Random samples from SST dataset.

Unconditional LD4LG Sample	Closest Training Instance
ruling spanking against Contentco is part of a legal battle that continues outside the European Commission ' headquarters.	The European Commission 's formal objections to the ContentGuard deal centered on the joint control that Microsoft and Time Warner would enjoy over an important player in the digital rights management industry.
Michael Phelps holds the all-around lead over American Michael Spinick, who has three Olympic gymnastics gold.	ATHENS (Reuters) - Michael Phelps led the United States to a narrow victory in the men's 4x200 meters freestyle relay at the Athens Olympics Tuesday to collect his third gold medal in four days.
A bill that would force doctors to delay their medical reports after surgery was close to gaining its way in the House of Representatives late Saturday.	Lawmakers at the Senate have delayed a controversial bill that would make it easier to sue online file-trading networks because there is too much opposition to it.
Desurgents in that rebel-held city include renewed air strikes against rebel positions in northern and northern areas.	With a US-led offensive on Falluja apparently imminent, rebels hit back with attacks in Samarra, Baghdad and Ramadi, another rebel-held city.
SeTwenty people were killed and more than 100 wounded when a bomb exploded late on Sunday in Thailand 's troubled Muslim province of Siam, the Human Medical Center (IRC) said.	Two people died and more than 20 others were injured when a bomb exploded at a Sungai Kolok bar Thursday night in Southern Thailand, The Nation reports.
BEIJING, Dec 11 (AFP) - World heavyweight champion Vitali Klitsch on Saturday began his fight for his first world middleweight title, making him look like a New York policeman.	10.25.04 - WBC Heavyweight Champion Vitali Klitschko will make his first title defense against the man who most recently knocked out Mike Tyson, Danny Williams, on Saturday, December 11, 2004, at the Mandalay Bay Resort amp; Casino in Las Vegas, Nev.
NEW YORK (Reuters) - Citigroup said on Wednesday it will buy Swedish law firm Charles Global Global Law Practice in a \$500 million deal that would \$3 billion a year. If the acquisition closes at \$2 per share, the acquisition would create the second firm	LONDON (Reuters) - U.S. investment bank Citigroup is set to bid for UK stockbroker Cazenove CAZ.UL, challenging rivals JP Morgan JPM.L and Lehman Brothers LEH.N for the City's most venerable institution, the Observer reported.
PHILADELPHIA – Ben Roethberger threw a pair of touchdown passes and came just closer to becoming his second straight Pro Bowl MVP, leading the Pittsburgh Steelers to a 28-10 victory over the Cincinnati Bengals that ended Cincinnati Bengals coach Bill Coughlin's 13-game winning streak.	IRVING, Texas - Ben Roethlisberger completed 21 of 25 passes and two touchdowns, leading the Pittsburgh Steelers to a 24-20 comeback win over the Dallas Cowboys.
Tokyo stocks ended mixed Monday morning as investors take profits from Wednesday's losses. The US dollar was higher against the yen.	Tokyo stocks ended mixed Tuesday as investors grew cautious ahead of the US presidential election. The US dollar edged higher against the Japanese yen.

Table 16: Random samples from AG News dataset. HTML entities are decoded and links are replaced with [link] for readability.

Conditional LD4LG Samples	
Positive	Negative
... begins the three series with a complex series of creepy characters and characters, a mystery we may not have seen from a mystery that we may or have never seen.	A non-mystery mystery.
The over overwrought melodrama John Byrne returns to a time-traveling tale that is in need by a man in a need to want his man trying to uncover what he gives.	A rather tired exercise in nostalgia.
Saucy has all the appeal of a romantic romantic comedy, but it lacks the energy of romance and a whole lot of the sassy sex and little of the fun.	A painfully flat exercise in down down flat storytelling.
It may not add up to the big budget, but it certainly gives it a trip worth taking a look at.	This is not original writing.
The gentle cartoon glides with humor, sensity and wryling wit.	If you're looking for a movie that gets under your skin, then you're in trouble of trouble.

Table 17: Random conditional samples from SST dataset.

Conditional LD4LG Samples			
World	Sports	Business	Sci/Tech
BBC.com's Mark Sutton looks back at the media frenzy which surrounds the European Commission chairman, Martin Schulz.	Reuters - Steelers linebacker Ben Brown will miss Sunday's game against the Buffalo Bills with a hamstring injury.	A new focus from Tuesday's event includes a press conference on a new research unit. Also: New customer training and development programs begin, as the company's founder heies to win on new customers. ip;, and more.	Japanese Space Agency has reported that the giant planet has about 20 times the size of Earth and is likely to be relatively quite bigger than Saturn's mysterious encircling planet, which is also known as Planck #39.
American swimmer Leah Leistman outfles Michael Schinberger, in the women's freestyle final.	After Florida played Oklahoma yesterday, no one in the game, but other teams are struggling struggling to get into the title title position. First one came: Florida's woeful 19-19 rout of No.	TOKYO (Reuters) - Tokyo's Nikkei average fell 0.14 percent by midmorning trade on Wednesday as falls in the extending of the day's decline in the wake of oil prices eased offset buying in blue-tech stocks amid concerns over supply prospects.	InfoWorld - Google has rolled out a beta beta version of the Google Desktop, a desktop search tool that enables people to search their computer hard drives and analysis the value of the applications on their traditional computers or Microsoft's PCs.
A proposal to give British families a time of living years after birth was due to gain strong backing in the House of Commons last night.	ATHENS (Reuters) - The United States thrashed Greece 85-75 to claim the sixth Olympic women's title Monday.	NEW YORK, October 27 (newratings.com) - Linux distributor Red Hat Inc (FRAT.ROAT.NAS) says it expects annual net income of \$500 million to \$8.5 million, up from \$5 in the previous quarter.	Reuters - International Business Machines Corp. has asked a bankruptcy judge to cancel its pension plan within days, increasing speculation the computer company may be losing ground in its billion-dollar pension plan.
The offensive on the entire rebel-held city includes an air strike on rebel positions each in a police station.	China has retained its gold medal at the fall Athens Olympics, taking Brazil one gold in all-around gymnastics.	In a rare end that the 17-month takeover battle between Oracle Corp. and SoftBank Group Corp, Oracle Corp has decided to make a \$10.7 billion tender offer for PeopleSoft Inc., ending a 17-figure battle.	MAST ST ST. HELENS, Wash., Oct. 20 - An earthquake antilock the magnitude of magnitude of Mount St. St Helens on Saturday, leading to lava explosions and a series of smaller earthquakes that erupted over the weekend causing to activity and sound in the area.
Se 19 people were killed and more than 100 wounded in a bomb blast late on Sunday in Thailand's troubled Muslim province of Atai, the Human Medical Center (IMC) said.	The lockout was announced it was already begun at Toronto Field Hockey Field today. It would probably be an historic moment for Toronto Rangers fans.	While Apple Computer has suffered through record strong music market growth over the past five months, the company's stock has been moving at a strategic strategy for years.	Nintendo Co.'s fourth generation of gaming systems based on the Nintendo DS and the Wii U/Lego mobile game platform will be released later this month, the company said Thursday.

Table 18: Random conditional samples from AG News dataset. HTML entities are decoded for readability.